Electrochemical Cell-Free Biosensors for Antibody Detection

Sara Bracaglia,[a] Simona Ranallo,[a],* Francesco Ricci [a],*

[a] Department of Chemistry, University of Rome, Tor Vergata, Via della Ricerca Scientifica, 00133 Rome, Italy
*Corresponding author: simona.ranallo@uniroma2.it; francesco.ricci@uniroma2.it
Supporting information for this article is given via a link at the end of the document.

Abstract: We report here the development of an electrochemical cell-free biosensor for antibody detection directly in complex sample matrices with high sensitivity and specificity that is particularly suitable for point-of-care applications. The approach is based on the use of programmable antigen-conjugated gene circuits that, upon recognition of a specific target antibody, trigger the cell-free transcription of an RNA sequence that can be consequently detected using a redox-modified probe strand immobilized to a disposable electrode. The platform couples the features of high sensitivity and specificity of cell-free systems and the strength of cost-effectiveness and possible miniaturization provided by the electrochemical detection. We demonstrate the sensitive, specific, selective, and multiplexed detection of three different antibodies, including the clinically-relevant Anti-HA antibody.

Introduction

Synthetic biology has recently emerged as the new frontier to develop sensors that can detect a wide range of targets with high sensitivity and specificity.[1] The possibility to use the enzymatic machinery of RNA transcription and protein translation in cell-free systems coupled with responsive synthetic genes has enabled to develop tools that are particularly promising for diagnostic and clinical applications.[2–6] Cell-free biosensors consist of rationally designed responsive gene circuits that, upon binding to a specific target, trigger the transcription/translation of a reporter molecule. Cell-free biosensors for the detection of specific nucleic acid sequences,[5–13] small molecules,[3,13–19] metal ions,[19–22] and biomolecules[23] including antibodies[24] have been reported to date demonstrating the possibility of using similar systems as analytical tools that are not only sensitive and specific but also rapid, low-cost and easy to use. The majority of these sensors employ as reporter species optically-active proteins (such as green fluorescent protein, GFP) or light-up RNA aptamers (such as spinach) that are respectively expressed or transcribed upon target recognition by the responsive gene circuit. While these examples present several advantages in terms of versatility and sensitivity, they remain bound to the limitations typical of optical methods: low performance in complex sample matrices (i.e., blood serum, whole blood, etc.) and not suitable for portable and low-cost instrumentation.

In response to the problems encountered by optical-based approaches, electrochemical platforms provide several advantages thanks to the low fabrication costs and operational convenience of modern microelectronics.[25,26] Moreover, electrochemical sensors can be mass-produced, require low sample volumes, are reusable, less prone to interference and, in conclusion, better suited for point-of-care applications than optical approaches.[27] Several electrochemical platforms have been reported to date for the rapid detection of antibodies showing high sensitivity, reproducibility, and multiplexing ability.[28–32] Despite these advantages, only a few reports have so far described the adaptation of cell-free biosensors with electrochemical detection.[2,15] In one clever demonstration, Pardee, Kelley and coworkers designed cell-free transcription/translation responsive gene circuits that, upon recognizing a specific RNA sequence, trigger the expression of a restriction enzyme that liberates a redox reporter-conjugated strand.[15] This strand can in turn be captured at the surface of a nanostructured microelectrode giving a measurable current signal. In another work, Pardee and coworkers coupled the classic RNA-responsive toehold switch cell-free biosensor with the well-known electrochemical glucose meter, one of the most widely available point-of-care sensing devices.[2] These examples perfectly highlight how the versatility of electrochemical detection coupled with the sensitivity and specificity of synthetic biology sensing strategies allow to achieve optimal analytical performances with low-resource experimental settings and multiplexing capabilities. Despite the above advantages, the electrochemical examples discussed above remain limited to the detection of RNA sequences and to the target-induced expression of a reporter enzyme. Developing responsive gene circuits that can be activated by a wide range of targets and could work with (easier to control) cell-free transcription-only systems would be crucial for the practical use of cell-free biosensors to meet diverse health challenges.

Motivated by the above considerations, we demonstrate here an electrochemical cell-free biosensor for the detection of specific antibodies (Anti-Dig, Anti-DNP, and Anti-HA antibodies) in blood serum. To do so, we designed antigen-conjugated gene circuits that respond to clinically-relevant target antibodies by triggering the cell-free transcription of an RNA sequence. This transcribed sequence, in turn, hybridizes to a redox-modified probe strand attached to an electrode generating a change in the measured electrochemical signal.[33]

Results and Discussion

Our strategy to achieve an electrochemical cell-free biosensor for antibody detection is based on an antibody-induced activation of a DNA gene circuit that transcribes for an RNA output sequence that can be successively detected by a disposable electrochemical sensor. The gene circuit is rationally designed to contain an incomplete T7 promoter domain that prevents efficient binding of the T7 RNA polymerase (T7-RNAP) enzyme and thus prevents efficient transcription of the RNA output strand.[34–36] To achieve antibody-induced activation of such gene circuit, we have designed a pair of antigen-

conjugated DNA input strands that can form a bimolecular complex only upon the bivalent binding of a target antibody to the two antigens. This bimolecular complex can efficiently hybridize to the single-strand portion of the gene circuit and reconstitute the promoter domain (Figure 1a). In the presence of T7-RNAP and the required nucleotides, the so-activated gene circuit leads to the efficient transcription of the RNA output strand (Figure 1b) that can be conveniently detected using a redox-labeled oligonucleotide probe site-specifically attached to a disposable interrogating electrode (Figure 1c).

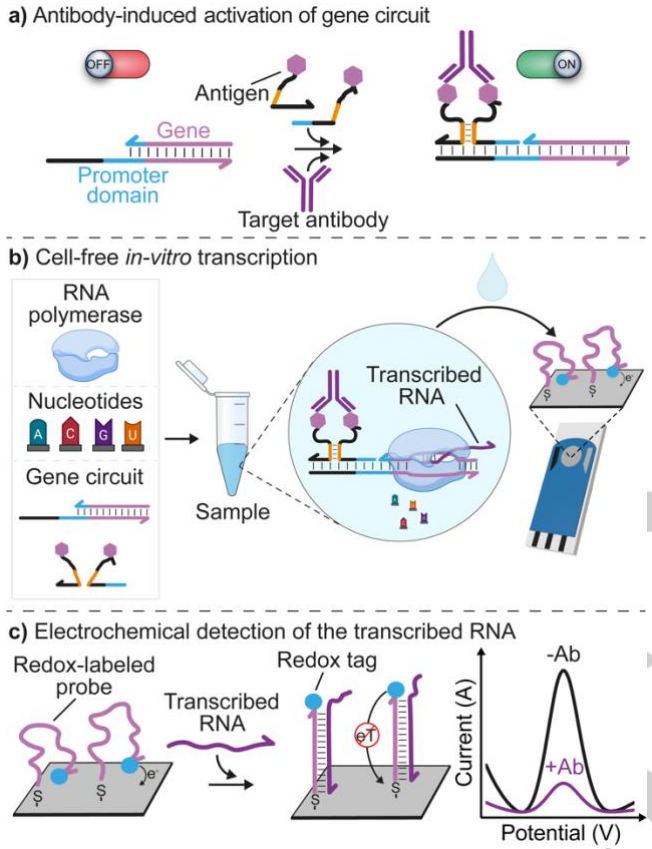

Figure 1. *Electrochemical cell-free biosensor for antibody detection. a) Antibody-induced activation of gene circuit. Two antigen-conjugated DNA strands can be co-localized upon binding to a target antibody and form a bimolecular complex that can hybridize to an inactive DNA gene circuit and activate it by reconstituting the complete T7-RNAP promoter domain. b) In the presence of T7-RNAP and the nucleotides, the so-activated gene circuit leads to the transcription of an RNA output strand. c) The transcribed RNA output sequence can be detected through an electrochemical sensor composed of a silver-based screen-printed disposable electrode on which a redox-labeled DNA probe strand complementary to the transcribed RNA strand is immobilized. The hybridization of the transcribed RNA strand leads to a decrease in the measurable electrochemical signal using square wave voltammetry (SWV).*

Our sensing strategy initially requires a rational design of the antigen-conjugated input strands that, upon bivalent binding of the target antibody, hybridize to the inactive gene circuit, and thus activate it (Figure 2a). To achieve this goal, it is instrumental to optimize the antigen-conjugated input strands so that they respect two main conditions. First, these strands should form a stable bimolecular complex through the hybridization of their complementary domains exclusively upon the antibody-induced co-localization.[37] Second, they should be programmed in a way so that at the concentrations employed in our experiments they will be able to hybridize to the inactive gene circuit only when they join into a bimolecular complex (i.e., each strand should not be able to bind to the gene circuit on its own).

As a first test bed to optimize the antigen-conjugated input strands we designed a set of strands with variable lengths of the input strands #1 and #2 that only when joined together can form the 21-nt strand complementary to the single-stranded portion of the inactive gene circuit. More specifically, we varied the length of the strand complementary to the single-stranded portion of the T7 promoter in the gene circuit (strand #1 in Figure 2b) from 5 to 19 nt. The length of the partner strand (strand #2 in Figure 2b) was varied accordingly to reach the total length of 21 nt. For these initial tests and to avoid possible confounder factors due to electrochemical heterogenous-phase systems, we have employed a gene circuit transcribing for a light-up fluorescent RNA aptamer (i.e., Mango). This 39-nt RNA aptamer binds to a thiazole orange (TO-1) increasing in its fluorescence signal.[38–40] The so-designed strands (strand #1 and strand #2) were then tested at a fixed equimolar concentration (300 nM) in the presence of the inactive gene circuit (100 nM) and a cell-free transcription mixture containing the TO-1 fluorophore and the fluorescent signal was recorded after 2 hours of transcription reaction.

First, we tested whether activation of the gene circuit can occur when the two input strands are separated. These experiments are aimed at understanding whether any leakage signal can occur in the absence of antibody co-localization. We observed low fluorescent signals (indistinguishable from that observed with the incomplete gene circuit alone) when using strand #1 with a length shorter or equal to 9 nt (together with strand #2 length from 12 to 16 nt). By increasing the length of strand #1 (> 9 nt) we observed an increase in the fluorescent signal likely due to the fact that hybridization of strand #1 to the gene circuit is enough to reconstitute the promoter domain (Figure 2c). For all these variants we also performed transcription experiments using a unimolecular control strand that results from joining together, through a duplex-forming stem, the two input strands (Figure 2c). These control experiments are aimed at understanding if the presence of the stem (that would result from joining together strand #1 and strand#2) in the activated gene can affect transcription. With such control strands, we observed efficient activation of the gene circuit (gray bars, Figure 2d) suggesting that the presence of the stem in the reconstituted synthetic gene does not affect transcription efficiency. Based on these results, for our next experiments on antibody-induced transcription, we selected the variant #4 which provides low leakage signal and a high transcription activation when the two strands are joined together (strand #1 - 11 nt, strand #2 - 10 nt).

Next, we move to the optimization of the system to achieve stable bimolecular complex formation of strand #1 and #2 upon bivalent antibody binding. To do that, we conjugated strands #1

and #2 with the small molecule hapten digoxigenin (Dig) and employed Anti-Dig antibody as our target. We also placed a spacer of 12-nt between the antigens and the stem-forming portions to allow more efficient antibody binding.[41–43] We have then designed a set of strand #1 and strand #2 couples each displaying a complementary stem-forming domain of variable length (from 0 to 16 nt) (Figure 1e). These two complementary portions should induce formation of the active bimolecular complex between strand #1 and strand #2 upon bivalent antibody binding to the two antigens. We performed transcription reactions in the absence and presence of Anti-Dig antibody (300 nM) for all the above-described strands. A complementary portion of 12-nt is the one that provides the greatest signal change between the absence and the presence of Anti-Dig antibody (Figure 2f). With shorter stem-forming length the antibody-induced co-localization is likely not enough to induce duplex formation between strand #1 and strand #2 and less efficient transcription is observed. On the contrary, at longer stem-forming lengths (>12 nt) we observe strong leakage signals likely because strand #1-strand #2 duplex forms even in the absence of the target antibody.

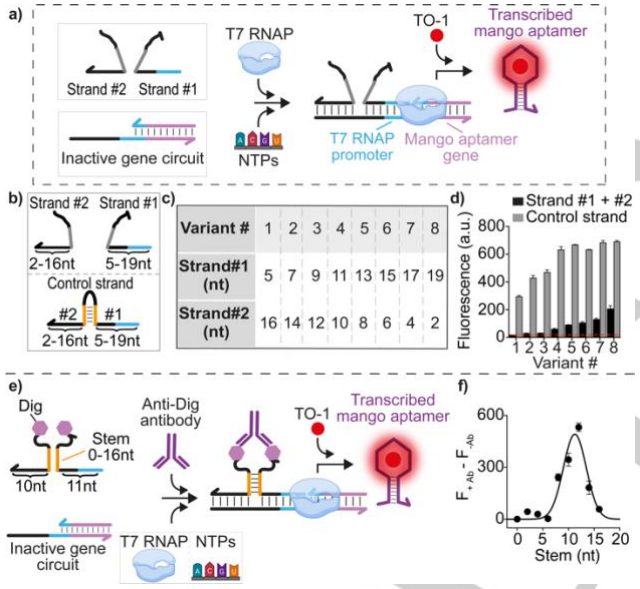

Figure 2. *Design and characterization of antibody-activated cell-free transcription. a) Scheme of cell-free biosensor designed to transcribe the light-up RNA Mango aptamer. b) Design of the variants with different lengths of the input strands #1 and #2 and of their corresponding control strand. c) Table of the different variants tested and the corresponding length of input strand #1 and #2. d) Fluorescence signal obtained with the different variants of input strands (black bars) and with their corresponding control strands (gray bars). e) Design of antigen-conjugated strands of variant #4 with different complementary stem lengths (ranging from 0 to 16 nt). f) Plot showing the difference between the fluorescence signals obtained in the presence ($F_{(+Ab)}$) (300 nM) and absence ($F_{(-Ab)}$) of Anti-Dig antibodies with Dig-conjugated DNA strands with variable lengths of the stem portions. Here the experiments were conducted at 37 °C in a 20 µL solution in presence of T7-RNAP (10 U/µL) and the required nucleotides (each at 10 mM) supplemented with inactive gene circuit (100 nM), the input strands (300 nM), the control strands (300 nM), the antigen-conjugated strands (each at 100 nM) and the Anti-Dig antibody (300 nM). The transcription reaction was allowed to proceed for 120 min and then an aliquot was transferred to 100 µL of 10 mM Tris-HCl and 75 mM KCl, pH 7.4 solution containing 200 nM of TO-1 and the fluorescence signal measured after 15 min at 545 nm. For these and the following experiments, the values represent averages of three separate measurements and the error bars reflect the standard deviations.*

With the above-described antibody-induced transcription reaction scheme and the optimized set of antigen-conjugated strands, we then moved to the demonstration of electrochemical antibody detection. To do so, we immobilized a 26-nt signaling DNA strand probe labeled at the 3' end with the redox label methylene blue and at the 5' end with a thiol group onto the surface of a disposable silver-based screen-printed electrode. Such signaling DNA probe is designed to be fully complementary to the antibody-induced transcribed RNA output strand. Hybridization event between the probe and the output RNA leads to a more rigid duplex that reduces the efficiency with which the terminal redox label collides with the electrode surface and transfers electrons, thus resulting in a lower Faradaic current (Figure 3a).

The disposable electrochemical sensor readily responds to the antibody-induced transcription reaction with excellent sensitivity and specificity. For example, the approach shows nanomolar sensitivities in both buffer (Figure S1, S2) and more complex samples (i.e., 20% bovine serum supplemented with increasing concentrations of Anti-Dig antibodies) with a dissociation constant (K_D) of 4.5 ± 0.5 nM and a limit of detection (LOD) of 1.5 nM (Figure 3b-c, S3a). A relative standard deviation (RSD%) of 7.9% was obtained with multiple measurements (n = 3) using different sensors at a fixed antibody concentration (30 nM). The platform is also highly specific, no measurable signal is observed in the presence of non-specific antibodies and with control experiments in which only one of the two input strands is employed (at 300 nM) (Figure 3d, S3b). The approach is modular and versatile and in principle generalizable to the detection of other antibodies. To demonstrate this, we have employed antigen-conjugated DNA strands with a different recognition element (i.e., dinitrophenol, DNP) and designed a second gene circuit inducing the transcription of an RNA sequence that binds to a second redox-labeled probe. With this new gene circuit, we have measured Anti-DNP antibodies reaching sensitivities (K_D = 3.6 ± 0.3 nM, LOD = 0.7 nM), reproducibility (RSD% = 3.2%), and specificities similar to those observed for the Anti-Dig antibodies (Figure 3e-g, S4).

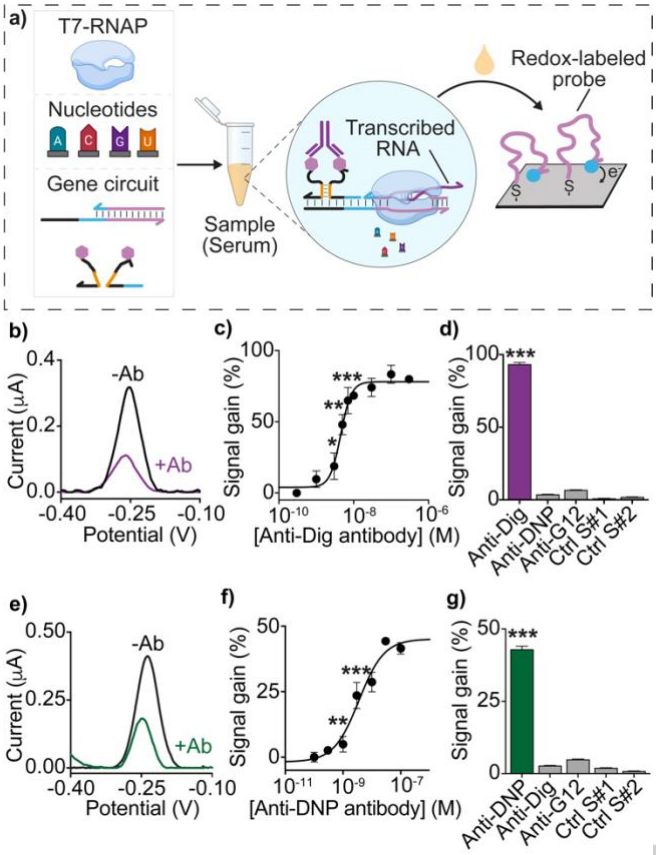

Figure 3. *Antibody detection using rationally designed cell-free biosensors. a) General scheme of our proposed electrochemical cell-free biosensor for antibody detection. b) SWV voltammograms obtained in the absence (black) and presence (purple) of Anti-Dig antibodies using the Anti-Dig cell-free biosensor. c) Signal gain values obtained at increasing concentrations of Anti-Dig antibodies, and d) at saturating concentration (300 nM) of Anti-Dig antibodies, non-specific antibodies, and with different control experiments. e) SWV voltammograms, f) dose−response curve, and g) specificity tests obtained using a cell-free biosensor for Anti-DNP antibody detection. The experiments were conducted at 37 °C in a 20 μL solution containing 20% bovine serum in presence of T7-RNAP (10 U/μL) and the required nucleotides (each at 10 mM) supplemented with inactive gene circuit (100 nM), the antigen-conjugated strands (each at 100 nM) and the antibodies as indicated. For these and the following experiments, the transcription reaction was allowed to proceed for 120 min and then an aliquot was transferred to 100 μL of 50 mM Na_2HPO_4 and 150 mM NaCl at pH 7.0 solution to the disposable electrode surface. SWV scans were performed between −0.4 and −0.1 V at 50 Hz after 120 min from the transfer of the solution on the electrode surface. For these and the following experiments, statistical analysis was performed with Prism GraphPad 9vs using two-tailed unpaired Student's t-test and the p-value ranges are indicated with black asterisks (*** < 0.001, ** = 0.001–0.01, * = 0.01–0.05).*

We then designed a modular version of the gene circuit that allows the use of a single antigen-conjugated strand designed to hybridize with two unmodified DNA strands. This modular version enables the use of peptide-PNA strands as recognition elements (Figure 4a). We tested the efficiency of such modular cell-free biosensor towards the detection of Anti-HA antibodies employing as recognition element a 9-residue epitope present in the hemagglutinin (HA) protein on the surface of influenza viruses.[44] Influenza epidemics have strong effect on society, including mortality, and economical consequences and so clinical assessment of influenza virus diseases and monitoring of immune responses to influenza vaccine or infection are needed.[45] The developed gene circuit for the clinically-relevant Anti-HA antibody detection reached sensitivities (K_D = 14.6 ± 0.1 nM; LOD = 2.9 nM), reproducibility (RSD% = 6.3%), and specificities (Figure 4b-c, S5-6) similar to those observed in the non-modular platforms. We have also evaluated the recovery percentages of spiked serum samples at four different Anti-HA concentrations (15, 25, 32, and 45 nM, n = 3 for each concentration) (Figure 4d). By replacing the measured current values of the spike sera samples in the equation obtained from the linear dynamic range (Figure S7) of the Anti-HA binding curve reported in Figure 4c, we calculated recovery percentages between 80% (at 25 nM Anti-HA concentration) and 119% (at 15 nM Anti-HA concentration) (Figure 4d).

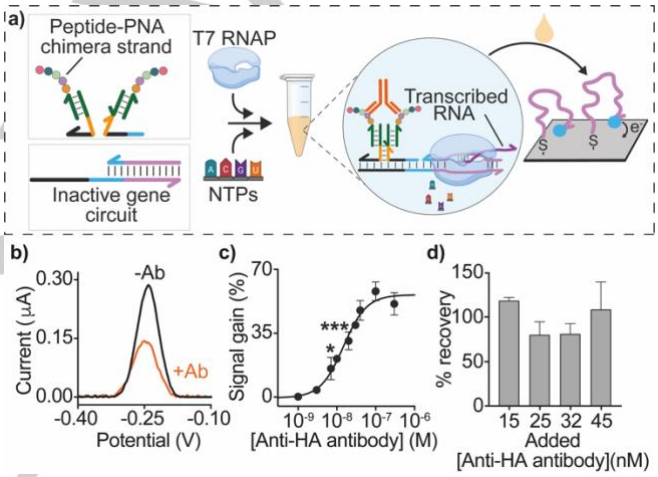

Figure 4. *Modular cell-free biosensor for clinically-relevant antibody detection. a) Modular design of a cell-free biosensor that employs peptide-PNA chimera strands to detect Anti-HA antibodies. b) SWV scans obtained in the absence (black) and presence (orange) of Anti-HA antibody concentration in a 20% diluted bovine serum solution. c) Signal gain values obtained at increasing concentrations of Anti-HA antibodies. c) Anti-HA antibody quantification assessed by spiking blank sera samples with different known concentrations of Anti-HA antibody (15, 25, 32, and 45 nM) shows a % of recovery from 80 to 119%. The experiments were conducted at 37 °C in a 20 μL solution containing 20% bovine serum in presence of T7-RNAP (10 U/μL) and the required nucleotides (each at 10 mM) supplemented with inactive gene circuit (100 nM), scaffold DNA strands (each at 80 nM), peptide-PNA chimera (240 nM) and the antibodies as indicated.*

The sensing approach presented here also supports the simultaneous measurement of two antibodies in a single sample solution. To demonstrate this, we have employed two gene circuits designed to transcribe for two distinct RNA output strands in response to two different antibodies (Anti-HA and Anti-DNP). We have also used a screen-printed electrode sharing the same reference and counter electrode but with two different working electrodes, each of which displays a redox-labeled DNA probe complementary to one of the two output

RNA strands. We mixed the two gene circuits in the same test tube and added various combinations of the two target antibodies (Figure 5a). The solution was then placed on the electrode surface and the current signal was measured for both probes separately. As expected, each gene circuit responds to its specific antibody generating a measurable reduction of the Faradaic current peak only in the corresponding working electrode (Figure 5b). The presence of the non-specific antibody causes only minimal signal for Anti-DNP sensor (sensor #1, -13% signal change) while no measurable signal was obtained with the Anti-HA sensor (sensor #2) in the presence of Anti-DNP antibody (Figure 5b).

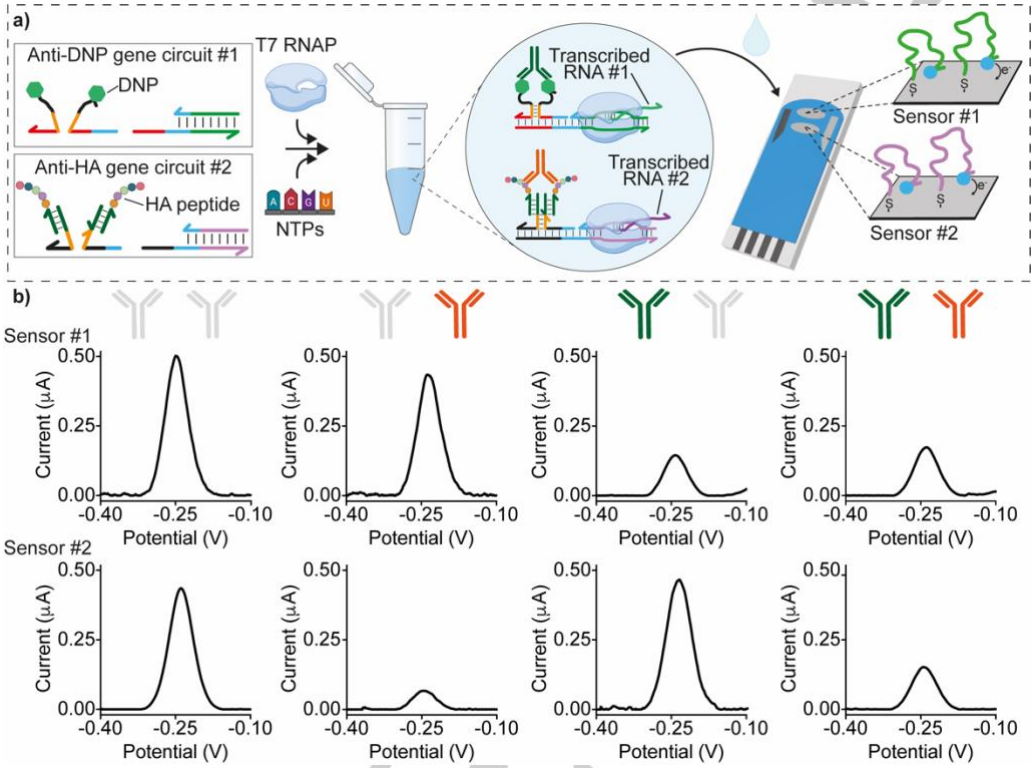

Figure 5. *Simultaneous detection of Anti-DNP and Anti-HA antibodies. a) Multiplex detection of Anti-DNP (green) and Anti-HA (orange) antibodies using two orthogonal cell-free biosensors in the same solution. After the transcription reaction, the solution was placed onto the surface of an electrode with two working electrodes each containing the redox-labeled probe specific for each gene circuit. b) SWV profiles achieved for different experiments with different combinations of both antibodies added to the solution. The colored antibody image identifies the added antibody for each experiment. The experiments were conducted at 37 °C in a 20 μL solution containing T7-RNAP (10 U/μL) and the required nucleotides (each at 10 mM) supplemented with inactive gene circuit (100 nM), the antigen-conjugated strands (each at 100 nM) or DNA scaffold strand (each at 80 nM)/Peptide-PNA chimera (240 nM) and the indicated antibodies (300 nM).*

Conclusion

In the present study, we report the development of an electrochemical cell-free biosensor for the detection of specific antibodies in blood serum. The approach is based on the use of programmable antigen-conjugated gene circuits that, upon recognition of a specific target antibody, trigger the cell-free transcription of an RNA sequence that can be consequently detected using a redox-modified probe strand immobilized to a disposable electrode. The platform is specific (no signal is observed with non-specific antibodies), sensitive (low nanomolar detection limit, well below the average serum levels of, for example, patients infected with influenza virus),[46] and versatile enough to be, in principle, adaptable to the detection of any antibody for which an antigen can be conjugated to a nucleic acid strand (although the effect of larger antigens on the co-localization and transcription efficiency still needs to be investigated). The approach we propose here maintains all the advantageous features of optical cell-free biosensors in which programmable responsive gene circuits have been employed for the detection of different targets (RNA sequences, small molecules, and antibodies).[6,19,24] These include the versatility of the approach and the easiness of experimental conditions together with high sensitivity and specificity. In addition to the above features, the electrochemical sensing scheme appears particularly suitable for point-of-care applications as it requires an inexpensive portable potentiostat, low-cost disposable sensors, and low sample volume. Moreover, since the electrochemical signal is promoted by the specific hybridization of the transcribed RNA output strand to the redox-labeled probe on the electrode, the approach can be employed even in complex samples. Finally, thanks to the possible miniaturization of the electrode surface, the high programmability of DNA-DNA interactions and the orthogonality of the responsive gene circuits the approach supports the detection of multiple antibodies

simultaneously. Our technology can be in principle adapted for the detection of different classes of antibodies (e.g., IgG, IgA, or IgM) by designing a specific gene circuit that can be activated only upon recognition of a specific antibody class. Phage-derived and HaloTag peptides can also be easily employed as recognition elements to widen the range of possible target antibodies.[28,29] The approach we propose here is convenient as it requires only inexpensive synthetic nucleic acid-modified strands and commercially available transcription kits. We estimate a cost of $0.5/test[47] in the current electrochemical detection scheme. Given all these advantages, electrochemical detection can emerge as a transduction mechanism of choice for the adaptation of cell-free biosensors in point-of-care diagnostic applications.

Acknowledgements

This work was in part supported by Associazione Italiana per la Ricerca sul Cancro, AIRC (project n. 14420) (F.R.), by the European Research Council, ERC (Consolidator Grant project n. 819160) (F.R.) and by the Marie Skłodowska-Curie grant agreement ("DNA-NANO-AB" project n. 843179) (S.R.).

Conflict of interest

The authors declare no conflict of interest.

Keywords: Electrochemical biosensors; Synthetic Biology; Antibody; DNA nanotechnology.

[1] K. E. French, *Nat. Sustain.* **2019**, *2*, 250–252.

[2] E. Amalfitano, M. Karlikow, M. Norouzi, K. Jaenes, S. Cicek, F. Masum, P. Sadat Mousavi, Y. Guo, L. Tang, A. Sydor, D. Ma, J. D. Pearson, D. Trcka, M. Pinette, A. Ambagala, S. Babiuk, B. Pickering, J. Wrana, R. Bremner, T. Mazzulli, D. Sinton, J. H. Brumell, A. A. Green, K. Pardee, *Nat. Commun.* **2021**, *12*, 724.

[3] S. Slomovic, K. Pardee, J. J. Collins, *Proc. Natl. Acad. Sci. USA* **2015**, *112*, 14429–14435.

[4] A. Tinafar, K. Jaenes, K. Pardee, *BMC Biol.* **2019**, *17*, 64.

[5] X. Tan, J. H. Letendre, J. J. Collins, W. W. Wong, *Cell* **2021**, *184*, 881–898.

[6] K. Pardee, A. A. Green, M. K. Takahashi, D. Braff, G. Lambert, J. W. Lee, T. Ferrante, D. Ma, N. Donghia, M. Fan, N. M. Daringer, I. Bosch, D. M. Dudley, D. H. O'Connor, L. Gehrke, J. J. Collins, *Cell* **2016**, *165*, 1255–1266.

[7] J. S. Gootenberg, O. O. Abudayyeh, M. J. Kellner, J. Joung, J. J. Collins, F. Zhang, *Science* **2018**, *360*, 439–444.

[8] K. Pardee, A. A. Green, T. Ferrante, D. E. Cameron, A. DaleyKeyser, P. Yin, J. J. Collins, *Cell* **2014**, *159*, 940–954.

[9] H. de Puig, R. A. Lee, D. Najjar, X. Tan, L. R. Soeknsen, N. M. Angenent-Mari, N. M. Donghia, N. E. Weckman, A. Ory, C. F. Ng, P. Q. Nguyen, A. S. Mao, T. C. Ferrante, G. Lansberry, H. Sallum, J. Niemi, J. J. Collins, *Sci. Adv.* **2021**, *7*, eabh2944.

[10] D. Ma, Y. Li, K. Wu, Z. Yan, A. A. Tang, S. Chaudhary, Z. M. Ticktin, J. Alcantar-Fernandez, J. L. Moreno-Camacho, A. Campos-Romero, A. A. Green, *Nat. Biomed. Eng* **2022**, *6*, 298–309.

[11] M. Karlikow, S. J. R. da Silva, Y. Guo, S. Cicek, L. Krokovsky, P. Homme, Y. Xiong, T. Xu, M.-A. Calderón-Peláez, S. Camacho-Ortega, D. Ma, J. J. F. de Magalhães, B. N. R. F. Souza, D. G. de Albuquerque Cabral, K. Jaenes, P. Sutyrina, T. Ferrante, A. D. Benitez, V. Nipaz, P. Ponce, D. G. Rackus, J. J. Collins, M. Paiva, J. E. Castellanos, V. Cevallos, A. A. Green, C. Ayres, L. Pena, K. Pardee, *Nat. Biomed. Eng.* **2022**, *6*, 246–256.

[12] M. M. Kaminski, O. O. Abudayyeh, J. S. Gootenberg, F. Zhang, J. J. Collins, *Nat. Biomed. Eng.* **2021**, *5*, 643–656.

[13] P. Q. Nguyen, L. R. Soenksen, N. M. Donghia, N. M. Angenent-Mari, H. de Puig, A. Huang, R. Lee, S. Slomovic, T. Galbersanini, G. Lansberry, H. M. Sallum, E. M. Zhao, J. B. Niemi, J. J. Collins, *Nat. Biotechnol.* **2021**, *39*, 1366–1374.

[14] A. D. Silverman, U. Akova, K. K. Alam, M. C. Jewett, J. B. Lucks, *ACS Synth. Biol.* **2020**, *9*, 671–677.

[15] P. Sadat Mousavi, S. J. Smith, J. B. Chen, M. Karlikow, A. Tinafar, C. Robinson, W. Liu, D. Ma, A. A. Green, S. O. Kelley, K. Pardee, *Nat. Chem.* **2020**, *12*, 48–55.

[16] J. K. Jung, C. M. Archuleta, K. K. Alam, J. B. Lucks, *Nat. Chem. Biol.* **2022**, *18*, 385–393.

[17] J. P. Hunt, J. Galiardi, T. J. Free, S. O. Yang, D. Poole, E. L. Zhao, J. L. Andersen, D. W. Wood, B. C. Bundy, *Biotechnol. J.* **2022**, *17*, e2100152.

[18] P. L. Voyvodic, A. Pandi, M. Koch, I. Conejero, E. Valjent, P. Courtet, E. Renard, J.-L. Faulon, J. Bonnet, *Nat. Commun.* **2019**, *10*, 1697.

[19] J. K. Jung, K. K. Alam, M. S. Verosloff, D. A. Capdevila, M. Desmau, P. R. Clauer, J. W. Lee, P. Q. Nguyen, P. A. Pastén, S. J. Matiasek, J. F. Gaillard, D. P. Giedroc, J. J. Collins, J. B. Lucks, *Nat. Biotechnol.* **2020**, *38*, 1451–1459.

[20] W. Thavarajah, A. D. Silverman, M. S. Verosloff, N. Kelley-Loughnane, M. C. Jewett, J. B. Lucks, *ACS Synth. Biol.* **2020**, *9*, 10–18.

[21] K. Beabout, C. B. Bernhards, M. Thakur, K. B. Turner, S. D. Cole, S. A. Walper, J. L. Chávez, M. W. Lux, *ACS Synth. Biol.* **2021**, *10*, 3040–3054.

[22] X. Lin, Y. Li, Z. Li, R. Hua, Y. Xing, Y. Lu, *RSC Adv.* **2020**, *10*, 39261–39265.

[23] Y.-J. Jang, K.-H. Lee, T. H. Yoo, D.-M. Kim, *Anal. Chem.* **2017**, *89*, 9638–9642.

[24] A. Patino Diaz, S. Bracaglia, S. Ranallo, T. Patino, A. Porchetta, F. Ricci, *J. Am. Chem. Soc.* **2022**, *144*, 5820–5826.

[25] M. Labib, E. H. Sargent, S. O. Kelley, *Chem. Rev.* **2016**, *116*, 9001–9090.

[26] Y. Yang, W. Gao, *Chem. Soc. Rev.* **2019**, *48*, 1465–1491.

[27] Y. Dai, C. C. Liu, *Angew. Chem. Int. Ed.* **2019**, *58*, 12355–12368.

[28] A. Valverde, A. Montero-Calle, B. Arévalo, P. San Segundo-Acosta, V. Serafín, M. Alonso-Navarro, G. Solís-Fernández, J. M. Pingarrón, S. Campuzano, R. Barderas, *Anal. Sens.* **2021**, *1*, 161–165.

[29] A. Montero-Calle, I. Aranguren-Abeigon, M. Garranzo Asensio, C. Povés, M. J. Fernandez-Aceñero, J. Martínez-Useros, R. Sanz, J. Dziaková, J. Rodríguez-Cobos, G. Solís-Fernández, E. Povedano, M. Gamella, R. M. Torrente-Rodríguez, M. Alonso-Navarro, V. de los Ríos, J. I. Casal, G. Domínguez-Muñoz, A. I. Guzmán-Aránguez, A. Peláez-García, J. M. Pingarrón, S. Campuzano, R. Barderas, *Engineering* **2021**, *7*, 1391-1412.

[30] S. S. Mahshid, F. Ricci, S. O. Kelley, A. Vallée-Bélisle, *ACS Sens.* **2017**, *2*, 718–723.

[31] S. Bracaglia, S. Ranallo, K. W. Plaxco, F. Ricci, *ACS Sens.* **2021**, *6*, 2442–2448.

[32] E. K. Leonard, M. Aller Pellitero, B. Juelg, J. B. Spangler, N. Arroyo-Currás, *J. Am. Chem. Soc.* **2022**, *144*, 11226–11237.

[33] F. Ricci, N. Zari, F. Caprio, S. Recine, A. Amine, D. Moscone, G. Palleschi, K. W. Plaxco, *Bioelectrochemistry* **2009**, *76*, 208–213.

[34] C. T. Martin, J. E. Coleman, *Biochemistry* **1987**, *26*, 2690–2696.
[35] M. Jiang, M. Rong, C. Martin, W. T. McAllister, *J. Mol. Biol.* **2001**, *310*, 509–522.
[36] J. Kim, K. S. White, E. Winfree, *Mol. Syst. Biol.* **2006**, *2*, 68.
[37] S. Ranallo, D. Sorrentino, F. Ricci, *Nat. Commun.* **2019**, *10*, 5509.
[38] J. Ouellet, *Front. Chem.* **2016**, *4*, 29.
[39] E. V. Dolgosheina, S. C. Y. Jeng, S. S. S. Panchapakesan, R. Cojocaru, P. S. K. Chen, P. D. Wilson, N. Hawkins, P. A. Wiggins, P. J. Unrau, *ACS Chem. Biol.* **2014**, *9*, 2412–2420.
[40] J. S. Paige, K. Y. Wu, S. R. Jaffrey, *Science* **2011**, *333*, 642–646.
[41] X. Zhang, L. Zhang, H. Tong, B. Peng, M. J. Rames, S. Zhang, G. Ren, *Sci. Rep.* **2015**, *5*, 9803.
[42] R. Luedtke, C. S. Owen, F. Karush, *Biochemistry* **1980**, *19*, 1182–1192.
[43] T. J. Smith, N. H. Olson, R. H. Cheng, E. S. Chase, T. S. Baker, *Proc. Natl. Acad. Sci. USA* **1993**, *90*, 7015–7018.
[44] D. Fleury, S. A. Wharton, J. J. Skehel, M. Knossow, T. Bizebard, *Nat. Struct. Biol.* **1998**, *5*, 119–123.
[45] T. Aydillo, A. Escalera, S. Strohmeier, S. Aslam, J. Sanchez-Cespedes, J. Ayllon, C. Roca-Oporto, P. Perez-Romero, M. Montejo, J. Gavalda, P. Munoz, F. Lopez-Medrano, J. Carratala, F. Krammer, A. García-Sastre, E. Cordero, *Cell Rep. Med.* **2020**, *1*, 100130.
[46] T. Yamazaki, J. Chiba, S. Akashi-Takamura, *Vaccines* **2018**, *6*, 35.
[47] B. Lavickova, S. J. Maerkl, *ACS Synth. Biol.* **2019**, *8*, 455–462.

Entry for the Table of Contents

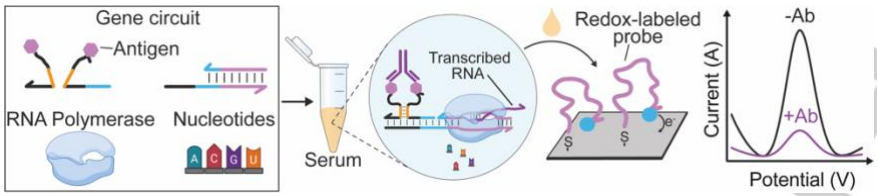

Table of Contents: We demonstrate the sensitive, specific, selective, and multiplexed detection of different antibodies in blood serum using electrochemical cell-free biosensors. The platform is based on programmable antigen-conjugated gene circuits that, upon recognition of a target antibody, trigger the transcription of an RNA sequence consequently detected with a disposable electrochemical sensor.

Institute and/or researcher Twitter usernames: @RicciLab @Simona_Ranallo @BracagliaSara